# Fast-Fourier-domain delay line for *in vivo* optical coherence tomography with a polygonal scanner

Amy L. Oldenburg, J. Joshua Reynolds, Daniel L. Marks, and Stephen A. Boppart

We demonstrate *in vivo* optical coherence tomography using a Fourier-domain optical delay line constructed with a commercially available polygonal scanner. The 20-faceted polygonal mirror array, capable of scanning at rates up to 15 kHz, is implemented at 4 kHz to acquire 500 × 500 pixel images at 8 frames/s with a signal-to-noise ratio of 80 dB. Features of this delay line include scalability to high repetition rates, 98.6% linearity in group delay over 2 mm, and bandwidth support exceeding 150 nm. Images are obtained in an animal model (*Xenopus laevis*), and limitations due to phase-delay nonlinearity and polygon asymmetry are discussed. © 2003 Optical Society of America

*OCIS codes:* 110.4500, 120.3180, 120.5800, 170.4500.

## 1. Introduction

Optical coherence tomography (OCT) is an imaging modality capable of resolving micrometer-scale features within living biological tissue.[1–5] One of the current technological challenges in OCT is to achieve real-time imaging rates with a minimal sacrifice in signal-to-noise ratio (SNR), resolution, and image size. We present a novel Fourier-domain delay line capable of real-time imaging that does not suffer from a trade-off between resolution and speed, which limits other designs. This delay line was constructed with a 20-sided commercially available polygonal mirror array. *In vivo* imaging is demonstrated, and practical considerations for the design and operation of the delay line are discussed.

OCT is implemented with a low-coherence light source and a Michelson interferometer as a heterodyne detector of backscatter from a reference and sample arm. A scanning reference arm is used to provide variable group delay, so that backscatter from the sample arm is gated to optically range a structure at varying depths within the sample. The phase velocity produced by the scanner determines the modulation frequency at the output of the interferometer, and electronic bandpass filtering is implemented to improve the SNR. In designing a reference arm delay line, one must consider several parameters, including the scan depth determined by the maximum group delay, the linearity of group delay to minimize distortion of the images, the cost and availability of components, the flatness of the optical response (in amplitude and phase) over the bandwidth of the light source, the repetition rate necessary for the desired image acquisition time, high duty cycle to improve SNR, and a modulation frequency compatible with available data-acquisition hardware. Often these parameters are conflicting, forcing a compromise of one for another. It is also important to note that, although the maximum scan rate is typically desired, an increase in speed requires a proportional increase in optical power to maintain the same SNR.[6]

In recent years there has been much interest in fast delay line designs for OCT.[6–15] The simplest delay line incorporates a translating retroreflector in the reference arm. Alternatively, a retroreflector can be mounted on a lever arm that is rotated through a small angle to create quasi-linear delay. Rapid periodic translation of a mirror is inhibited by its mechanical inertia as the scan rate is increased. The practical limitation to such a device with a scan range of 3 mm is ~100 Hz. An increased scan rate can be achieved with a piezoelectric transducer to stretch a spool of optical fiber, achieving up to 600 Hz for a similar path delay.[7] However, stretching hysteresis, dynamic changes in birefringence, and sensitivity to temperature drift reduce the consistency of the

The authors are with the Department of Electrical and Computer Engineering, Beckman Institute for Advanced Science and Technology, University of Illinois at Urbana-Champaign, 405 North Mathews, Urbana, Illinois 61801. S. A. Boppart's e-mail address is boppart@uiuc.edu.

Received 11 November 2002; revised manuscript received 27 February 2003.

0003-6935/03/224606-06$15.00/0

achievable delay. A further increase in scan rate can be achieved with a continuously rotating device. A spinning cube delay line[8,9] uses internal reflections from the cube surfaces to produce angle-dependent group delay. Although scan rates up to 28.6 kHz have been reported,[9] these systems suffer from high nonlinearity in group delay because of the cube geometry, forcing a trade-off between larger size (decreased nonlinearity) and scan rate. A scan rate of 2.58 kHz was achieved with the combination of a commercially available polygonal mirror array (similar to the one used in this study) and a parallelepiped,[10] but this system also suffers from high group-delay nonlinearity. A rotating prism array with internal reflection was demonstrated at 2 kHz.[11] It exhibits improved group-delay linearity (99%); however, the prism array is highly customized, and OCT imaging was not demonstrated. In all the above-mentioned devices, with the exception of the translating mirror, the optical path length through glass elements varies over the scan, causing variable group-velocity dispersion (GVD), which can be detrimental to the axial resolution. This problem can be partially alleviated, however, if the sample has similar dispersive properties as the glass element.[11] One scanner design that does not exhibit any of these difficulties is based on a rotating mirror array[12] that was demonstrated at 2.4 kHz with a scan range of 2 mm. Currently this device appears to be untested on *in vivo* samples, and a drawback is that the mirror array is highly customized. Recently, a 2-kHz scanner was described that uses a multipass cavity to generate large group delays by translating one of the cavity mirrors by a small amount.[13] However, at 1 kHz and a 1.4-mm imaging depth, this scanner exhibits group-delay nonlinearity (<10%). In addition, parasitic modulation (<10%) arises because of beam fluctuations during actuation of the scanner.

Fourier-domain delay lines, developed from femtosecond pulse-shaping technology, achieve a linear group delay by applying a linear phase to the pulse in the Fourier plane of the pulse shaper. In this way, a variation in the reflection angle of a mirror placed in the Fourier plane can be used to produce time delay. The advantage of this design is that the group and phase delay can be tuned independently. One implementation consists of a periodically tilting mirror driven by a galvanometer[14] or a resonant scanner,[6] achieving axial scan rates up to 4 kHz for a maximum group delay of 3 mm. However, it is necessary to keep the mirror size small because of inertial considerations, which limits the maximum optical bandwidth that the device can support for a given scan depth and modulation frequency. Axial resolution in OCT is inversely proportional to optical bandwidth, implying a trade-off between resolution and speed for these devices. A new type of scanner was recently demonstrated by Lee *et al*,[15] who used two frequency comb generators with offset modulation frequencies to produce depth scanning at 500 kHz without mechanical motion. However, the comb generators are of limited span in frequency, so that the maximum achievable resolution was ~100 μm.

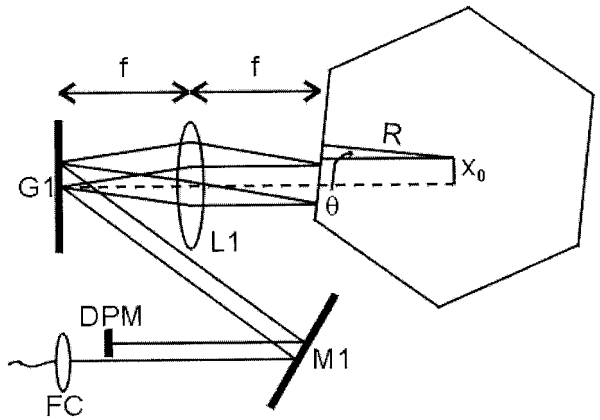


Fig. 1. Schematic of a Fourier-domain delay line with a polygonal mirror array. Although a 20-sided polygon is used in this study, a 6-sided array is illustrated for clarity. FC, fiber collimator; DPM, double-pass mirror; M1, steering mirror; G1, grating; L1, achromatic lens. $R$ is the inner radius of the mirror array, θ is the scan angle, $f$ is the focal length of the achromat, and $x_0$ is the offset of the pivot point of the mirror array from the optical axis.

In this paper we describe a Fourier-domain delay line that is scalable to higher speed without limiting the mirror size due to the fact that the delay element is a rotating polygon mirror array. It is typically linear in group delay, and, as with other Fourier-domain delay lines, its phase delay (and hence modulation frequency) can be adjusted independently. There is some nonlinearity in the phase delay because of the geometry of the polygon, which causes chirp in the modulation signal. Since the chirp in the modulation frequency is linear, it should be straightforward to compensate for it digitally so that this delay line can be used for phase-sensitive applications such as Doppler OCT. It is also necessary to implement corrections because of the asymmetry in construction of these commercial polygonal mirror arrays, which are addressed in Section 2. Many of the fast delay lines reviewed above[8–12,15] are currently untested with *in vivo* OCT imaging. We successfully acquired OCT images using this delay line at 4 kHz in a living tadpole (*Xenopus laevis*) at real-time frame rates.

## 2. Polygonal Delay Line Design

The basic design of a double-pass Fourier-domain delay line with a polygonal mirror array as the delay element is shown in Fig. 1. The advantage of a double-pass design is twofold: The amount of group delay is doubled and the transverse displacement of the beam over the scan angle can be counteracted. Light from the fiber interferometer is collimated and directed toward a grating where it is reflected at normal incidence to minimize GVD.[6,14] The angularly dispersed light is then imaged onto the surface of a polygon mirror by an achromatic lens. Dispersion caused by passage through the lens glass can be compensated by tuning the distance between the lens and

the grating. To lowest order, the size of the image on the mirror is given by

$$\text{image size} \approx \frac{f\Delta\lambda}{d}, \tag{1}$$

where $f$ is the lens focal length, $\Delta\lambda$ is the optical bandwidth in wavelength units, and $d$ is the pitch of the grating. The light is then reflected from the scanning mirror where it travels back through the system to the double-pass mirror and is retroreflected. Analyzing the geometry of the polygon mirror as it is rotated an angle $\theta$ (in radians) from the normal gives the following expression for phase delay:

$$l_p(\theta) = 4[x_0 \tan\theta - R(1 - \sec\theta)] \approx 4x_0\theta + 2R\theta^2, \tag{2}$$

where $x_0$ is the offset of the pivot point of the mirror array from the optical axis and $R$ is the inner radius of the mirror array. The first term is the result for a tilting mirror system[6,14]; however, a nonnegligible correction term $2R\theta^2$ arises from additional translation of the mirror because of the pivot arm length $R$. The group delay is given by the expression

$$l_g(\theta) \approx 4x_0\theta + 2R\theta^2 - \frac{4f\lambda_0\theta}{d}, \tag{3}$$

where $\lambda_0$ is the center wavelength of the light source. The last term in approximation (3) is the contribution from the mirror tilt that applies a linear phase ramp in the Fourier domain. For most practical applications, this last term will dominate.

Using the designs of Eqs. (1) and (2) and approximation (3), one can determine the optimal choice of lens, grating, mirror size, pivot offset $x_0$, and total scan angle for the desired application. Typically a scan depth of 2–3 mm is chosen for OCT imaging because of the limited penetration depth of singly scattered near-infrared light in scattering tissue. From approximation (3), the maximum scan depth into the sample (which is only half of the group delay because the light must travel in and out of the sample) is $2f\lambda_0\theta_m/d$, where $\theta_m$ is the maximum scan angle swept by the polygon. Since the duty cycle is proportional to $\theta_m$, it is desirable to maximize it by choosing a lens with the shortest possible focal length. A large-aperture lens is usually chosen for flexibility to prevent clipping over the range of the scan. To this end, an achromat with $f = 50$ mm and a diameter of 30 mm was chosen for this study. With $\lambda_0 = 800$ nm and $1/d = 600$/mm, the scan angle necessary to achieve 2 mm of optical delay is 2.4°. For this system, a bandwidth of 150 nm was desired to accommodate the full spectrum of the light source. By use of Eq. (1) the corresponding image size on the mirror is 5 mm. The polygonal mirror array is then chosen such that the facets are sufficiently wide to accommodate the image over the scan angle, also accounting for the pivot offset $x_0$ and aerodynamic believing of the polygon edges. Since it is desirable

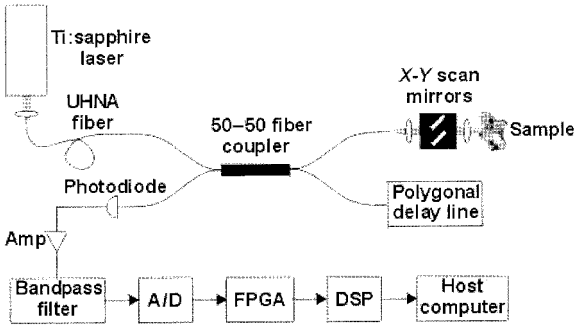


Fig. 2. Schematic of the fast OCT system used for testing the performance of the Fourier-domain polygonal mirror delay line. The signal is converted with an analog-to-digital (A/D) converter and subsequently processed with a field-programmable gate array (FPGA) and digital signal processor (DSP) before display on the host computer.

to minimize the nonlinear terms in Eq. (2) and approximation (3) by keeping $R$ small, and since it is desirable to have a large number of facets $n$ to maximize the repetition rate, the facet size $[2R\tan(\pi/n)]$ should be chosen to be as small as possible. Ultimately it is these nonlinear terms that limit the design of this system. Fortunately, it is not difficult to achieve high group-delay linearity with typical design parameters. For this study a 20-sided mirror array with a facet width of 10 mm and $R = 31.75$ mm was selected. The nonlinearity $\approx R\theta_m d/4f\lambda_0$ is then expected to be 1.4% over the 2-mm scan depth.

The central modulation frequency for this device, which is determined by the phase velocity, can be written as

$$f_{\text{mod}} = \frac{1}{\lambda_0}\frac{\partial l_p}{\partial t} \approx \frac{4\omega}{\lambda_0}(x_0 + R\theta), \tag{4}$$

where $\omega$ is the rotational velocity of the mirror. The implication of the $R\theta$ term is that the modulation frequency varies over the scan, imparting a chirp to the detection signal. However, this is not the same as optical chirp due to GVD, which is dependent on sample composition and can be detrimental to the axial resolution. Instead, the consequence of this term is to place greater requirements on the bandwidth of the detection electronics. For example, in the research presented here, a rotational velocity of 200 revolutions/s results in ~8-MHz variation in $f_{\text{mod}}$ over the desired 2-mm scan depth. This should be accounted for in addition to the optical bandwidth $\Delta\lambda$, which requires $\Delta\lambda(\partial 1_g/\partial t)/{\lambda_0}^2$ of detector bandwidth.[6] The offset $x_0$ can then be chosen to center $f_{\text{mod}}$ at the desired frequency.

### 3. Experiment

We tested the performance of the polygonal delay line using the fast OCT system illustrated in Fig. 2. The light source consists of a femtosecond Ti:sapphire oscillator that pumps an ultrahigh numerical aperture (UHNA) fiber[16] to produce 60 mW of optical power with a FWHM bandwidth of 70 nm centered at 800

nm. This is fusion spliced onto the input arm of a 50–50 fiber coupler (Gould Fiber Optics, Millersville, Md.) where the light is then split into the reference and sample arms of the interferometer. The sample arm consists of a fiber collimator, two orthogonal galvanometer-controlled mirrors for scanning in the transverse plane, and a 50-mm focal-length lens. Interference from the reference and sample arm is measured by a p-i-n photodiode at the output arm of the interferometer. The electronic signal is subsequently amplified, bandpass filtered with a passband of 1–5.5 MHz, digitized to 12-bit precision, then sent to a field-programmable gate array (FGPA) and digital signal processor (DSP) for processing and display on the host computer. The maximum axial scan rate is limited to a computer transfer rate of 4 Mbytes/s over the peripheral component interconnect bus. This limits our axial scan rate to 4000 axial scans per second for 500 × 500 pixel images at 8 frames/s.

The delay line consists of a fiber collimator, a grating with 600 line pairs/mm blazed at 800 nm, and an achromatic doublet with a focal length of 50 mm and a diameter of 30 mm. The mirror array and corresponding motor and control electronics were manufactured by Lincoln Laser Corp., Phoenix, Arizona. The polygonal mirror array has 20 facets of a 10-mm width and an inner radius of 31.75 mm. The motor (Model SA34) is capable of speeds up to 45,000 rpm, corresponding to a maximum axial scan rate of 15 kHz. The double-pass mirror and fiber collimator are mounted together on a linear translation stage for adjustment of the total optical path length. The lens and mirror array are also mounted on a common translation stage so that GVD can be adjusted by tuning the lens–grating separation.

We measured the SNR of this system by placing a retroreflecting mirror in the sample arm and measuring the voltage ratio between the maximum signal and the noise floor. With 20 mW of optical power at the sample and a 4-kHz axial scan rate, the SNR was measured to be 80 dB. In comparison, the shot-noise-limited SNR under these conditions, accounting for estimated signal loss due to the limited passband of the electronics, fiber coupling and grating inefficiencies, and increased background due to fiber end reflection in the sample arm,[17] is estimated to be 91 dB. An analysis of the receiver noise (including two amplifier stages) indicates that it contributes <2% to the total noise measured. Optical source noise (also known as excess photon noise) may arise in this system because of the impulsive noise of the periodic pulse train produced by the Ti:sapphire mode-locked laser, which can subsequently be amplified by the nonlinear optical processes inherent to continuum generation within the UHNA fiber. This source of noise could be reduced in future implementations by use of dual-balanced detection.

We experimentally verified group-delay linearity by placing a retroreflecting mirror on a translation mount in the sample arm. Light from a diode laser was obliquely reflected off an unused portion of the polygon and into a photodetector to generate a trigger signal to synchronize computer data acquisition with mirror position. As the mirror was translated and the scanner was operated at 4 kHz, the time delay between the center of the interference pulse and the reference signal was measured. The results are plotted in Fig. 3 in terms of the scan angle that is equal to the time delay multiplied by the rotational velocity of the polygonal mirror array (ω). As shown by comparison of the data with the best-fit line, the group delay is linear to within an experimental error (<5%). There was no meaningful curvature because of the nonlinear term in approximation (3), which would be 2% at a mirror position of ±1500 μm. The measured scan velocity is 62 m/s, which also matches the calculated value.

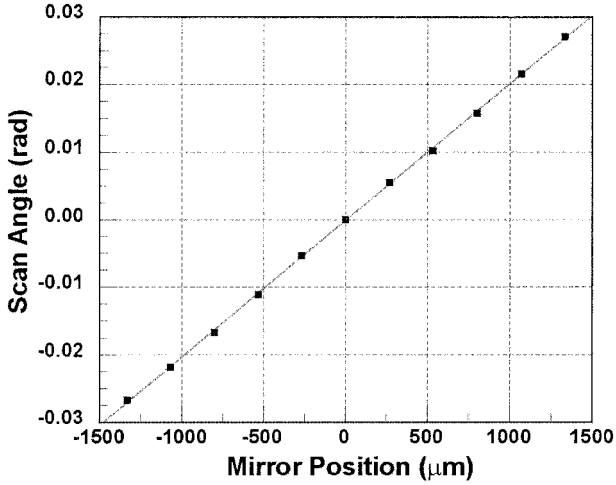

Fig. 3. Polygonal scanner angle versus sample arm mirror position. A best-fit line is shown to illustrate the linearity.

A typical interferogram, obtained by placing a mirror in the sample arm, is shown in Fig. 4. The spectrum, shown in the lower plot of Fig. 4, has a central frequency of 2.5 MHz with a bandwidth of 1.8 MHz. A shift to higher frequencies was noted as the sample mirror was translated away from scan center ($\theta = 0$), as would be expected from Eq. (4). The limited passband of the detection electronics (1–5.5 MHz), however, tended to clip the response for larger translations (>0.75 mm) from center. It is also important to note that, as with any high-speed OCT system, significant bandwidth support is required to achieve the desired axial resolution. For this experiment, with a 70-nm optical bandwidth at 800 nm, the axial resolution will be 4 μm in air, which corresponds to a 13-MHz bandwidth for the group velocity of this scanner. However, the measured axial resolution for fast scanning was larger than the ideal value (~12 μm). We verified this value using a slowly scanning system that did not exhibit electronic clipping, indicating that aberration in the lens (likely due to chromatic effects) is the limiting factor to the resolution. However, an estimate of the effects of electronic clipping occurring at fast scanning rates would suggest that the resolution will be broadened

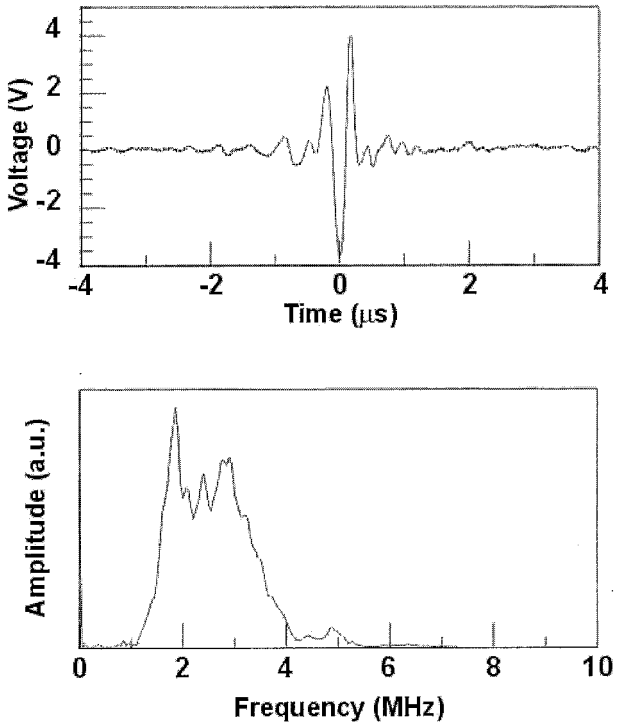


Fig. 4. Interferogram obtained from a mirror surface while axial scanning at 4 kHz with the polygonal delay line. The associated spectrum is plotted in the lower panel.

to a similar value of 12 μm in the absence of lens aberration.

To demonstrate the performance of this commercial mirror array, an OCT image of a coverslip surface is shown in Fig. 5(a). Because of machining variations in the tilts and distances of the polygonal facets from the rotational center, each facet produced a slightly different group-delay offset. Distortion due to the ±25-μm tolerance in the mirror facets can be seen at higher magnifications. This distortion is in the form of a 20-pixel repeating pattern corresponding to a slightly varying group delay imparted by each mirror facet. This could be a result of a variation in $R$, or in the horizontal tilt causing a shift in $\theta$. Using the information from the image of an optical flat, one can easily compensate for this offset by translating each axial scan line a known amount, as shown in Fig. 5(b). This correction was also applied to subsequent *in vivo* images in postprocessing, and in the future it should be straightforward to implement in real time. However, there are some additional effects that should be noted that arise because of asymmetries in the array. A change in the vertical tilt of a facet will slightly misalign the beam as it returns to the fiber coupler, resulting in a variation in the observed contrast. Careful study of Fig. 5(b) reveals this effect: The coverslip appears to have a repeating pattern of light and dark across its surface. It may be possible to correct for this effect by generating a contrast profile for each mirror facet. Finally, it was observed that one of the 20-mirror facets exhibited a significantly degraded resolution (by a factor of 2). This particular facet was also found to have a larger amount of group-delay offset (~20 μm) with respect to the other facets (corrections ranging over ±10 μm). One possible explanation is that the facet is translated too far from the focus of the lens, imparting GVD that degrades the resolution. If so, it implies that operation of the scanner over larger angles may result in a degradation of the resolution because of the translation term $4x_0\theta + 2R\theta^2$. For this system, the practical imaging range therefore can be limited to ~2 mm. It is interesting to note, however, that this degradation due to GVD may also be a problem for other Fourier-domain scanners employing a tilting mirror because the $4x_0\theta$ term can be significant.

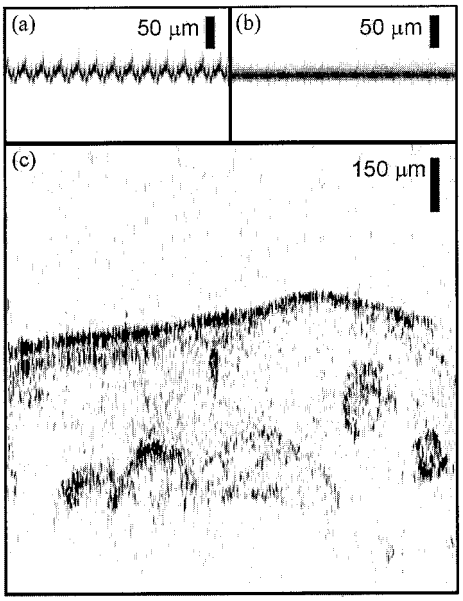


Fig. 5. OCT images acquired with the polygonal delay line at 8 frames/s and 500 × 500 pixels. Images (a) and (b) were cropped for illustration. (a) Raw image of coverslip surface. (b) Image of coverslip surface after correction for mirror offsets. (c) Image acquired from the dorsal side of a *X. laevis* tadpole, after correction.

Real-time performance of the polygonal scanner was tested by OCT imaging of live African frog tadpoles (*X. laevis*). The care and handling of these specimens was under the approved protocols of the University of Illinois at Urbana-Champaign Institutional Animal Care and Use Committee. These tadpoles were in later stages of development (stage 53, day 24) and were significantly more opaque than those typically used as models for OCT imaging. An anesthetized tadpole was placed in a small petri dish and positioned with a three-axis stage in the sample arm. The OCT beam was scanned across the long axis of the tadpole. The power incident on the tadpole was limited to 10 mW to prevent injury. Operating the polygonal scanner at 4 kHz, 500 × 500 pixel images were obtained at a frame rate of 8 Hz. One such image is illustrated in Fig. 5(c), after corrections for the group-delay offsets were applied. (These corrections were performed blindly once the factors were determined by analysis of the coverslip image.) It

appears that features within the tadpole can be resolved at depths up to 0.4 mm below the surface; however, given the high frame rates available, it may be possible to observe deeper features by averaging. It is also reassuring that the resolution of these features appears to be maintained over the scanning range.

## 4. Conclusion

We have presented a novel Fourier-domain delay line for OCT using a polygonal mirror array that is commercially available. Because it uses a rotating delay element, it is scalable to higher repetition rates without compromise to the mirror size (imaging resolution). In this study, scanner rotation rate was reduced to generate axial scan rates at 4 kHz because of hardware limitations. However, the polygon can be rotated to produce axial scan rates up to 15 kHz with its current motor. It is highly linear in group delay (98.6% over 2 mm), exhibits a SNR of 80 dB, and GVD is expected to be negligible over this scan range. Nonlinearity in the phase velocity may put greater requirements on the bandwidth of the detection electronics. However, using a passband of 1–5.5 MHz, we obtained real-time imaging in an animal model where features could be observed 0.4 mm into the tissue. An upgrade to higher-bandwidth electronics, as well as a digitally implemented nonstationary filter designed to compensate for the frequency-swept Doppler carrier, should increase the performance of this scanner, and a polygon with a smaller radius may be desired in future implementations to reduce the nonlinear effects. Using this scanner, we have further developed the potential for high-speed real-time OCT imaging of *in vivo* biological systems.

We acknowledge the technical contributions of Alex Schaefer for the development and programming of the real-time FPGA and DSP-based OCT acquisition system. This research was supported in part by funding provided by the National Science Foundation (BES-0086696), the Whitaker Foundation, and the Beckman Institute for Advanced Science and Technology. Correspondence can be directed to boppart@uiuc.edu or through http://nb.beckman.uiuc.edu/biophotonics.

## References

1. D. Huang, E. A. Swanson, C. P. Lin, J. S. Schuman, W. G. Stinson, W. Chang, M. R. Hee, T. Flotte, K. Gregory, C. A. Puliafito, and J. G. Fujimoto, "Optical coherence tomography," Science **254,** 1178–1181 (1991).
2. G. J. Tearney, M. E. Brezinski, B. E. Bouma, S. A. Boppart, C. Pitris, J. F. Southern, and J. G. Fujimoto, "*In vivo* endoscopic optical biopsy with optical coherence tomography," Science **276,** 2037–2039 (1997).
3. S. A. Boppart, G. J. Tearney, B. E. Bouma, M. E. Brezinski, J. F. Southern, and J. G. Fujimoto, "Noninvasive assessment of the developing *Xenopus* cardiovascular system using optical coherence tomography," Proc. Natl. Acad. Sci. USA **94,** 4256–4261 (1997).
4. S. A. Boppart, B. E. Bouma, C. Pitris, J. F. Southern, M. E. Brezinski, and J. G. Fujimoto, "*In vivo* cellular optical coherence tomography imaging," Nat. Med. **4,** 861–864 (1998).
5. B. E. Bouma and G. J. Tearney, eds., *Handbook of Optical Coherence Tomography* (Marcel Dekker, New York, 2001).
6. A. M. Rollins, M. D. Kulkarni, S. Yazdanfar, R. Ungarunyawee, and J. A. Izatt, "*In vivo* video rate optical coherence tomography," Opt. Exp. **3,** 219–229 (1998), http://www.opticsexpress.org.
7. G. J. Tearney, B. E. Bouma, S. A. Boppart, and B. Golubovic, "Rapid acquisition of *in vivo* biological images by use of optical coherence tomography," Opt. Lett. **21,** 1408–1410 (1996).
8. F. Lindgren, R. Gianotti, R. Walti, R. P. Salathe, A. Haas, M. Nussberger, M. L. Schmatz, and W. Bachtold, "−78-dB shot-noise limited optical low-coherence reflectometry at 42-m/s scan speed," IEEE Photon. Technol. Lett. **9,** 1613–1615 (1997).
9. J. Szydlo, N. Delachenal, R. Gianotti, R. Walti, H. Bleuler, and R. P. Salathe, "Air-turbine driven optical low-coherence reflectometry at 28.6-kHz scan repetition rate," Opt. Commun. **154,** 1–4 (1998).
10. N. Delachenal, R. Walti, R. Gianotti, S. Christov, P. Wagner, R. P. Salathe, U. Durr, and G. Ulbers, "Robust and rapid optical low-coherence reflectometer using a polygon mirror," Opt. Commun. **162,** 195–199 (1999).
11. M. Lai, "Kilohertz scanning optical delay line employing a prism array," Appl. Opt. **40,** 6334–6336 (2001).
12. N. G. Chen and Q. Zhu, "Rotary mirror array for high-speed optical coherence tomography," Opt. Lett. **27,** 607–609 (2002).
13. P.-L. Hsiung, X. Li, C. Chudoba, I. Hartl, T. H. Ko, and J. G. Fujimoto, "High-speed path-length scanning with a multiple-pass cavity delay line," Appl. Opt. **42,** 640–648 (2003).
14. G. J. Tearney, B. E. Bouma, and J. G. Fujimoto, "High-speed phase- and group-delay scanning with a grating-based phase control delay line," Opt. Lett. **22,** 1811–1813 (1997).
15. S.-J. Lee, B. Widiyatmoko, M. Kourogi, and M. Ohtsu, "Ultrahigh scanning speed optical coherence tomography using optical frequency comb generators," Jpn. J. Appl. Phys. **40,** L878–L880 (2001).
16. D. L. Marks, A. L. Oldenburg, J. J. Reynolds, and S. A. Boppart, "Study of an ultrahigh-numerical-aperture fiber continuum generation source for optical coherence tomography," Opt. Lett. **27,** 2010–2012 (2002).
17. A. G. Pololeanu, "Unbalanced versus balanced operation in an optical coherence tomography system," Appl. Opt. **39,** 173–182 (2000).